

MIT Open Access Articles

*Simultaneous transverse loading and axial strain
for REBCO cable tests in the SULTAN facility*

The MIT Faculty has made this article openly available. **Please share**
how this access benefits you. Your story matters.

Citation: Fry, Vincent, Estrada, Jose, Michael, Philip C, Salazar, Erica E, Vieira, Rui F et al. 2022. "Simultaneous transverse loading and axial strain for REBCO cable tests in the SULTAN facility." Superconductor Science and Technology, 35 (7).

As Published: 10.1088/1361-6668/AC6BCC

Publisher: IOP Publishing

Persistent URL: <https://hdl.handle.net/1721.1/148291>

Version: Author's final manuscript: final author's manuscript post peer review, without publisher's formatting or copy editing

Terms of use: Creative Commons Attribution-Noncommercial-Share Alike



Simultaneous transverse loading and axial strain for REBCO cable tests in the SULTAN facility

Vincent Fry^{1**}, Jose Estrada¹, Philip C. Michael¹, Erica E. Salazar^{1**}, Rui F. Vieira¹, Zachary S. Hartwig¹

¹ MIT Plasma Science and Fusion Center, 167 Albany St, Cambridge MA, 02139, USA

E-mail: vfry@psfc.mit.edu

Received xxxxxx

Accepted for publication xxxxxx

Published xxxxxx

Abstract

We present the design and first results of an assembly that enables Rare Earth Barium Copper Oxide (REBCO) superconducting cables –the VIPER cable in this work – to be tested in the SULTAN facility under the simultaneous application of transverse electromechanical loading and axial mechanical strain. The objective is to emulate the loads that a REBCO cable would experience in a three-dimensional coil but in shorter and simpler straight cables, reducing the cost, schedule, and complexity of high-fidelity conductor qualification. The assembly uses two methods for inducing axial strain in the cables. First, hydraulic jacks stretch the assembly and inserted Invar shims lock in up to ~0.3% axial cable strain on the benchtop at room temperature. Second, the different coefficients of thermal expansion between Invar clamps and the copper cable are exploited to induce an additional ~0.3% axial strain on the cable when the sample is cooled in the SULTAN test well from room temperature to below 50 K. FEA modeling shows that the soldered matrix of the VIPER cable transfers approximately 50-60% of the external cable strain into the REBCO stack. The assembly was successfully employed at SULTAN, enabling two VIPER cables to be cycled 500 times at 382 kN/m transverse electromechanical loads with ~0.5% mechanical strain on the cable (corresponding to ~0.3% mechanical strain in the REBCO stacks) demonstrating critical current degradation stabilizing after 30 cycles at less than 5% and providing confidence in VIPER cables under realistic high-field magnet conditions.

Keywords: VIPER cables, REBCO, critical current degradation, SULTAN

1. Introduction

Many high-current cable configurations utilizing rare-earth-barium-copper-oxide (REBCO) coated conductors are under development for large-scale, next-generation, high-field magnet applications [1]–[7]. Magnetic confinement fusion devices, in particular, benefit greatly from the use of REBCO-based cables because they offer the possibility of magnets operating in excess of 20 tesla peak field-on-coil. Such high-field operation enhances fusion performance over moderate-field devices using low temperature superconductor (LTS) magnets, permitting substantial reduction in device size

because of favorable, non-linear scalings with magnetic field strength [8], [9].

Although the strain sensitivities of individual REBCO tapes to tension, torsion, and bending have been widely investigated (e.g. [10]–[14]), predicting and measuring the strain sensitivity of critical current in REBCO-based cables is still an active area of research and development. Electromagnetic loads on cables within a magnet typically manifest in two orthogonal directions: (1) hoop tension along the conductor axis (parallel to current flow) and (2) transverse loading in the radial direction of the coil (perpendicular to current flow). For high-field REBCO magnets, the mechanical strains resulting from hoop tension can exceed 0.2% while the

** Vincent Fry and Erica Salazar are now at Commonwealth Fusion Systems.

mechanical body loads from transverse electromagnetic loading can approach 1000 kN/m. As such, it is highly desirable to test cable samples with both loads applied simultaneously during critical current measurements. Because such tests are generally performed using straight cable sections for practical reasons, it would be advantageous if hoop tension could be emulated as axial strain in straight cable samples rather than in a more complex 3D winding or full-scale magnet. While transverse Lorentz ($I \times B$) loading can be achieved by placing a cable with current (I) in an external magnetic field (B), emulating hoop tension via axial loading has been historically more difficult to achieve.

The FBI facility at Karlsruhe Institute of Technology was developed to evaluate whether the critical current performance of LTS cables under axial load corresponded to that extrapolated from individual conductor strands [15]. The facility was recently upgraded to support similar testing of high temperature superconductor (HTS) cables such as REBCO [16]. Testing under controlled axial load is the focus of the FBI measurements and conductor samples are tested individually. The sample is connected to a static load frame in liquid helium bath at the low end and, through a low-heat-leak pull rod, to a room temperature hydraulic actuator at its upper end. To maintain axial alignment between the upper and lower sample terminals, the transverse $I \times B$ loads that invariably arise in this configuration are reacted against a closely-spaced lateral support. Although transverse loading of samples under test is present, it is not a major emphasis for the facility. Due to the facility's limited peak current and the need to employ flexible current connections at the top of the sample, it is infeasible to replicate the high $I \times B$ loads expected in high-field REBCO magnets.

During the past decade, the principal focus of the SULTAN facility at Paul Scherrer Institut has been the qualification of ITER Nb_3Sn conductors and joints [17]. SULTAN employs a hairpin sample configuration (e.g. two parallel straight cables connected by a "U" shaped bottom joint), rigidly connected at its upper end to a high-current capacity superconducting transformer. This configuration is ideally suited to provide moderate- and high-field magnet relevant transverse $I \times B$ loading via an external magnetic field. High transverse loading on one sample leg is reacted against that on the other, with no net transverse loading on the sample. The SULTAN facility also serves as a general purpose LTS [18] and HTS [19] cable test facility.

The axial strain achieved in LTS cable samples generally arises due to thermal contraction mismatch between the cable and its structural jacket. A representative case study is the testing of Nb_3Sn cables for the ITER toroidal field (TF) and central solenoid (CS) magnets. In early tests, however, the unanticipated relaxation of axial cool-down strains due to cable slippage inside cable-in-conduit (CIC) samples towards the SULTAN high-field zone resulted generally poor

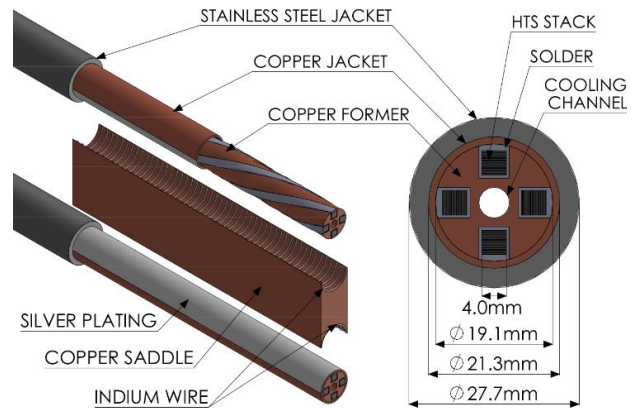


Figure 1: An example of a joint between VIPER cables as tested in SULTAN: A copper saddle joint between two VIPER cables (left); A cross section of a single VIPER cable, showing the VPI soldered stacks within channels in the copper former surrounding a central cooling channel

extrapolation of SULTAN sample data to in-coil performance [20], [21]. The introduction of crimp rings in the jacket of SULTAN samples, which mechanically interlock the cable axial strains in place, was implemented to preserve the proper strain and has since yielded significant improvement in predicted performance [22]; however, there remain concerns about the fidelity and extent to which straight cable samples can emulate the strain magnitude and distribution that occur in a coiled cable as a result of hoop tension [17]. The authors are aware of only a single experimental effort to induce strain in straight cables – Nb_3Sn in this case – that were tested in SULTAN; however, in this case the samples were strained at room temperature before $I \times B$ loading with the experiment yielding inconclusive results that were never published [23]. Clearly, as shown here, careful attention to detail as well as the design of the cables and structural assembly for SULTAN must be shown in order to properly produce the axial strain necessary to emulate the hoop tension in straight cable tests.

In this paper, we present an experimental method to characterize the critical current performance of VIPER (Vacuum pressure solder impregnated, Insulated, Partially transposed, and Roll-formed) REBCO cable-in-conduit (CIC) cable in the SULTAN facility under simultaneous, controlled, mechanically-applied axial strain and electromechanically applied transverse load at relevant magnitudes for high-field VIPER-based magnets operating in excess of 20 tesla. The method relies on two features: (1) the design of the cable assembly to enable the application of axial strain approaching $\sim 0.6\%$ of the external jacket of the VIPER cables and (2) the unique soldered nature of the VIPER cable, which mechanically bonds the REBCO stack and effectively transfers the external strain on the jacket to the individual REBCO tapes. The paper is laid out as follows: Section 2 reviews the VIPER cable design; Section 3 presents the design of the cable test assembly for SULTAN; Section 4 presents the

experimental tests results for the test at SULTAN; and Section 5 concludes with a summary.

2. Overview of VIPER cable

VIPER cable is based on the high-temperature superconductor cable architecture known as Twisted Stacked Tape Conductor (TSTC) first proposed by Takayasu *et al.* [24]. In the TSTC configuration, REBCO tapes are stacked to jointly handle the large electrical currents required for superconducting magnets and twisted to provide partial transposition to mitigate AC losses. Bending the twisted cable prior to the solder process permits magnet fabrication with minimal strain accumulation within the REBCO tapes. A cut-away schematic of a VIPER cable and cable-to-cable electrical joint developed specifically for superconducting tests at the SULTAN facility [18] is shown in Figure 1.

The cable comprises a central leak-tight channel carrying cryogenic coolant in a copper core. Rectangular channels on the perimeter helically twist around the central channel at a twist pitch of 20 cm and support the HTS stacks. A copper jacket extending axially over the cable and joint regions is compacted around the central assembly, providing mechanical support for the internal HTS stacks, an electrically conductive shell for current transfer, and a vacuum tight seal for a vacuum pressure impregnation (VPI) solder process, which mechanically, thermally, and electrically bonds all components of the cable together. To achieve additional mechanical support against $I \times B$ loading, the copper-jacketed cable can either be inserted directly into a steel radial plate or can have a steel jacket compacted around the copper jacket as shown in Figure 1. Strong, low resistance termination joints or cable-to-cable joints are easily created by clamping around the copper jacket, removing a short section of stainless-steel jacket if necessary. An overview of fabrication, cryostability, and mechanical and thermal cycling performance of VIPER cable can be found in [1] while an overview of voltage and fiber optic quench detection on VIPER cable can be found in [25].

The cable VPI soldering is especially germane to creating axial strain in straight VIPER cables. The solder process creates a uniform metal matrix of all components in the cable, mechanically bonding the REBCO tapes, the copper core, and the copper jacket together. As a result, externally applied stress to the copper jacket along the cable axis is transferred to the REBCO stack, inducing uniform axial strain in the individual REBCO tapes that is approximately 50-60% of the axial strain induced on the exterior cable copper jacket, as shown in Section 3. Thus, if a method can be developed to ensure constant applied stress to the copper jacket of VIPER cables during testing in SULTAN, testing on straight cables will include both the $I \times B$ transverse loading as well as the axial strain to emulate hoop tension.

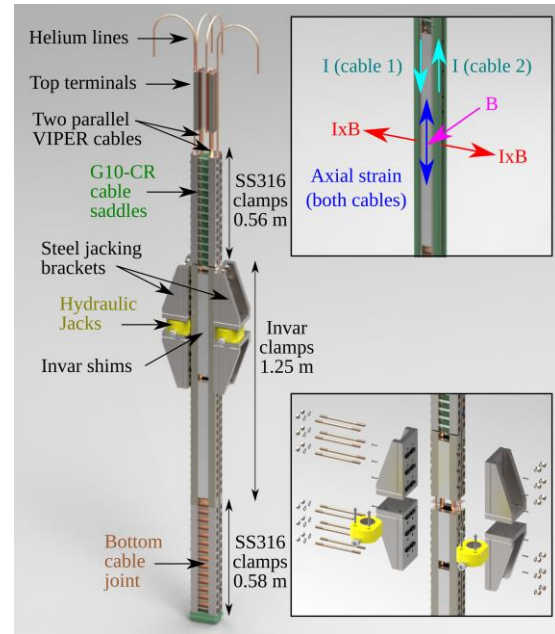


Figure 2: The cable assembly enclosing two VIPER cables for testing at SULTAN. The top-right inset describes the $I \times B$ and strain directions on the cables; the bottom-right inset shows how the strained assembly with hydraulic jacks is assembled.

Two VIPER cables were fabricated for the test at SULTAN under axial strain, which was denoted the “Charlie” test. The cables were fabricated with one stack of 96 REBCO tapes in a channel in the copper former. This was done to (1) match the cable current in the previous unstrained cable test at SULTAN denoted “Bravo” for a direct comparison [1] and (2) to keep the cable critical currents at a practical level (<60 kA) for flexible experiments at SULTAN. The remaining three channels were filled with identical stacks of SS304 “dummy” tape, which was required to enable the REBCO stack to experience uniform axial strain. The stainless-steel jacket shown in Figure 1 was omitted to reduce axial strain forces.

3. Design and qualification of the assembly

This section describes the design of the cable assembly, both the standard SULTAN assembly features and the innovations to enable the application of axial strain to the REBCO stacks, as well as the instrumentation scheme and initial benchtop tests.

3.1 Overview of the assembly design

The overall design of the cable test assembly, which is shown in Figure 2, hews closely to the “standard” assembly that has been developed over many years at SULTAN for ITER Nb_3Sn and $NbTi$ cables. The following “standard” features enable transverse $I \times B$ loading of the two cables within the SULTAN test well:

- **Cables:** Two cables measuring approximately 2.95 m length are oriented in a parallel configuration, referred to as the “right” and “left” leg.
- **Joints:** There are two types of joints composed of oxygen free high conductivity (OFHC) copper (e.g. C101): (1) the top terminals connecting the cables to the SULTAN facility’s HTS adapter; and (2) the bottom cable-to-cable joint.
- **Cooling lines:** External brazed copper cooling lines transfer supercritical helium between 4 and 50 K at 10 bar between the cables and the SULTAN cryogenic system.
- **Clamps:** Machined stainless-steel (e.g. SS316) clamps extending the length of the assembly that compress the cables and react the large $I \times B$ forces.
- **Insulation:** Cables are separated from each other, the steel clamps, and the SULTAN test well walls using high-strength cryogenic insulator materials (e.g. G10-CR or G11-CR) in the shape of saddles and shims.
- **Hardware:** Silver-plated stainless-steel (e.g. SS316) nuts, washers, bolts, etc. that compress the cables and insulation and rigidly supports electromagnetic loads during testing.

3.2 Assembly modifications to enable axial strain

To emulate the magnitude of hoop-tension-induced strain in cables found in high-field REBCO coils (typically 0.3% or less), the following enhancements to the standard test assembly were made to enable axial strains approaching 0.6%:

1. **Enhanced friction coatings in clamps:** The machined inner grooves of the clamps, which contact the cables in the joint regions, were tungsten carbonite spray coated to increase the coefficient of static friction between the cable jacket and steel clamps from 0.2 (steel clamp on steel jacket) to 0.8 (steel clamp on copper jacket), ensuring axial strains approaching 1% could be reached without slippage.
2. **Extended bottom joint:** To further increase the retaining force on the cables as they are strained, the bottom joint was elongated from the 400 mm joints used for other VIPER tests at SULTAN to 580 mm to maximize the tungsten carbonite spray coated area in contact with the cables. While this places the bottom joint closer to the high-field test region, adding magnetoresistance, the higher contact area for current transfer largely offsets this effect. [1]
3. **Hydraulic jack and shim compatibility:** The clamps were modified to enable the connection of one pair of steel brackets on each side of the assembly. In between each bracket pair, an Enerpac SRS500TB hydraulic jack rated for 50 tons can be placed. The jacks expand in the axial direction, straining the cables through the clamps and creating gaps between the clamps near the

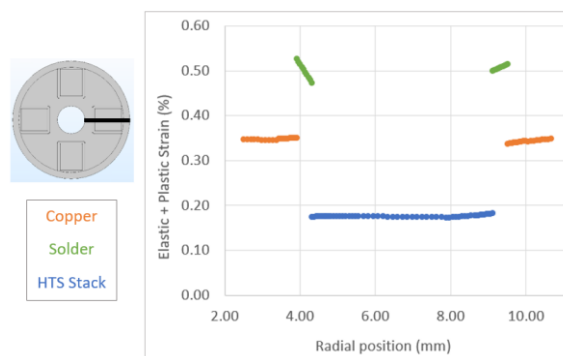


Figure 3: FEA results for differential CTE-induced strain in a VIPER cable when cooled from 297 K to 20 K. The x axis of the figure corresponds to horizontal line shown on the cross section. The axial strain is into/out of the page.

center of the assembly. Custom machined Invar shims can then be inserted between neighboring clamps to retain the desired strain after the jacks and brackets are removed for insertion into the SULTAN test well. The hydraulic method, applied first in the assembly process, provided approximately 0.3% external axial strain on the benchtop before insertion of the assembly into the SULTAN test well.

4. **Selective use of Invar for clamps:** The difference in the cumulative coefficients of thermal expansion (CTE) between the copper cable (0.33% from 293 K to 20 K) and Invar (0.04% from 293 K to 20 K) was exploited to provide an additional axial strain when the test assembly is cooled from room to cryogenic temperatures. The central set of clamps (labeled in Figure 2 and shaded light grey in Figure 4) were made of Invar while the clamps on each end nearest the top and bottom joints were made of SS316, the CTE of which largely matches copper. The differential CTE strain remains essentially constant below 50 K.

Figure 3 shows the results of a Finite Element Analysis (FEA) model of straining a VIPER cable via the differential CTE of the clamps in the assembly. In this model, a single cable is fixed in position at both ends and the model is cooled from 297 K to 20 K. As described in Figure 2, the VPI solder process creates a solid metal matrix which transfers the external strain on the jacket to strain on the REBCO stack; however, the REBCO stacks only accumulate approximately half of the external axial strain on the jacket. All interfaces are assumed bonded, which has been confirmed visually with destructive tests of previous cable samples. In this model, isotropic material properties of the REBCO stack were used for simplicity. Inclusion of anisotropic effects, which derive from the decreased stiffness in the radial direction of the stack due to the copper and solder components of the REBCO stack, would result in shear leading to slightly non-uniform strain

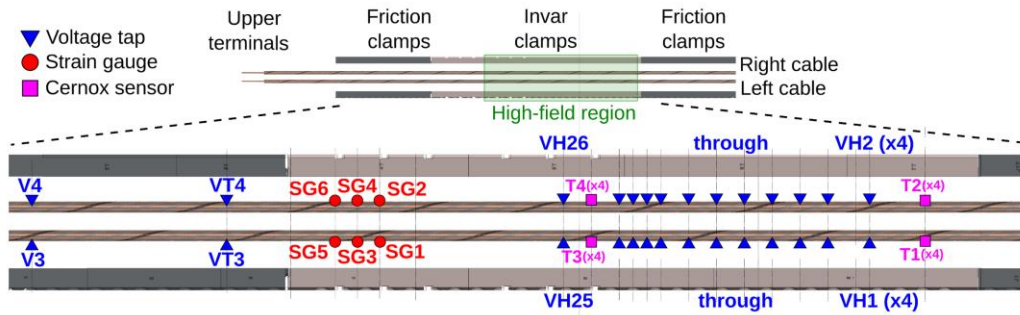


Figure 4: The instrumentation map for the strained cable assembly at SULTAN

distribution in the radial direction of the tape stack. For the purposes of these experiments, the differential strain across the tape stack is negligible compared to the total strain and was not necessary in the analysis.

3.3 Instrumentation scheme

Similar to the assembly itself, the instrumentation applied to the right and left cables was extended beyond the standard set of temperature and voltage sensors to properly verify the axial strain of the cables during assembly and testing. Figure 4 provides a graphical overview of the instrumentation scheme. Sensors of a given type are labelled sequentially along the sample, starting from the bottom joint. Odd-numbered sensors denote the left cable while even-numbered sensors were applied to the right cable.

Sensors beginning with “VH” are voltage taps applied at 25 mm to 100 mm intervals along the high field test region to monitor the effect on measured critical current of the orientation of the REBCO tape stack with respect to the background field. The voltage taps labelled “VT” and “V” confirm the lack of anomalous voltages elsewhere along the sample and help to measure the resistance of the joints from the facility current terminals to the upper ends of the sample legs. Sensors beginning with “TS” are Cernox® temperature sensors located below and above the high field test region that monitor the sample temperature during critical current and temperature sharing measurements. They can be used to calorimetrically confirm power generation during these measurements. The “(x4)” notation indicates that four sensors were placed at this axial location but spread evenly around the azimuth of the cable at 90° intervals.

All voltage taps and temperature sensors were installed by the SULTAN technical staff following arrival of the cables and test assembly at the facility. Confirmation of sensor integrity was performed during cooldown and the initial zero current tests before the test campaign began.

Sensors beginning with “SG” are strain gauge half bridges that monitored the strain state of the cables during pre-test benchtop mechanical loading and during intra-test cooldown cycles. Each half bridge contained one active and one dummy gauge. Templates were used to position the

MicroMeasurement 125 BZ gauges within ± 6 mm at a nominal distance of 1608 mm from the bottom of the sample, avoiding both the sample’s clamps and the Teflon spacers that were used to set the distance between the centerlines of the sample conductors. The gauges were mounted using MicroMeasurement AE-15 adhesive, which was cured using resistive heaters mounted to either side of the instrumented section.

The strain gauges were mounted to the outer surface of the conductor’s copper jacket. Two of the active gauges on each cable (denoted SG1 and SG5 for the left cable, SG2 and SG6 for the right cable) were nominally centered over and aligned angularly to follow the twist pitch of the REBCO stack. The third strain gauge on each cable (denoted SG3 on the left cable and SG4 on the right cable) was mounted above the copper former and aligned parallel to the conductor axis. This was done to measure the different axial strains induced in the copper jacket when over solid copper cable former and over the groove in the cable former which the REBCO stack was soldered. The dummy gauges were mounted to a 150 mm long section of spare VIPER cable using the same arrangement relative to the tape stack as the corresponding active gauge. The dummy conductor was loosely held between the two active conductors and was free to thermally contract.

Upon completion of the sample assembly at MIT, the performance of the strain loading and strain monitoring systems were verified by straining the cables on the bench top. The sample, with clamps and hydraulic jacks installed, was placed on supports, with the cabling to the strain gauge bridges connected to a MicroMeasurements® MM8000 strain gauge readout for continuous monitoring during hydraulic loading.

3.4 Initial benchtop strain results

The overall displacement of the conductor legs was monitored both by dial indicators located at both ends of the sample, as well as optically, by measuring the displacement of lines scribed onto the surfaces of the conductor jackets near the friction clamps. The displacement of the scribed lines divided by the distance between verified the recorded strain gauge readings. The displacement of the scribe lines relative to the friction clamps confirmed analysis which showed that

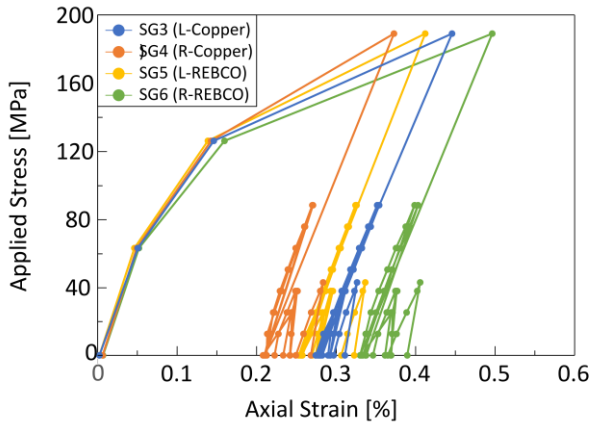


Figure 5: Measurements for the initial three room-temperature strains of the cable assembly with the hydraulic jacks at MIT.

as the frictional force on the cable builds up, the cable gradually displaces approaching the leading edge as it is strained to its final value over a length of ~ 200 mm. This slippage can reduce average cable strain by $\sim 0.1\%$ compared to a case with bonded ends.

Figure 5 shows the measured stress-strain curve during the first three hydraulic loading cycles of the sample. The vertical axis was obtained from the recorded hydraulic pressure in the jacks, multiplied by their piston areas and divided by the cross-sectional areas of the conductor legs. The first loading cycle, from 0% to $\sim 0.4\%$ strain, resulted in plastic deformation of conductors, primarily due to annealing of the copper former and jacket during the VPI solder process. It is important to note that plasticity is present because stainless-steel jackets were not used on this sample. This was done to reduce the loading required to strain the cable and to ensure proper load transfer between the friction clamps and cable. Cables to be used in high field magnets would employ either stainless steel jackets or radial plates to reduce or eliminate this plasticity. Strain gauges SG1 and SG2 were lost and positional inaccuracy of the gauges can explain the $\sim 0.05\%$ difference in measured strains seen.

In preparation for shipping to SULTAN, the stress was removed from the cables by removing the Invar shims. Analysis indicates that approximately $\sim 0.3\%$ and $\sim 0.1\%$ residual axial strain remained in the jacket and REBCO stacks, respectively, due to the plastic deformation that occurred in the unintentional overstressing that occurred on the first benchtop test. This is evident in Figure 5, which shows the first loading to $\sim 0.4\%$ followed by a relaxation of the stress and two subsequent stress cycles.

4. Experimental results at SULTAN

Upon arrival at SULTAN, instrumentation (e.g. voltage taps, Cernox sensors, etc.) was added to the cables. Multiple

low strain cycles were then carried out to verify the assembly was ready for installation in SULTAN. During the final cycle, Invar shims were installed to ensure no gaps were present between invar clamps in the axial direction. The hydraulic jacks and brackets were then removed and the sample was installed into the SULTAN test well.

The primary testing objective was to evaluate the potential for critical current degradation resulting from the combination of transverse lateral loads and axial strain. To isolate the effect from strain, results from strained test (named “Charlie” test) could be compared to an identical set of unstrained cables tested under identical electromagnetic conditions (named “Bravo” test). The SULTAN testing program was structured as follows:

1. Cool down to 5 K and strain gauge verification
2. Instrumentation check and current ramps at $B=0$ T
3. Baseline DC characterization ($B=10.9$ T, $T=10$ K)
4. IxB cycling to 100 cycles (35 kA \times 10.9 T = 382 kN/m)
5. Reference DC characterization ($B=10.9$ T, $T=10$ K)
6. Intentional quench of sample
7. Reference DC characterization ($B=10.9$ T, $T=10$ K)
8. IxB cycling to 500 cycles (35 kA \times 10.9 T = 382 kN/m)
9. Reference DC characterization ($B=10.9$ T, $T=10$ K)
10. Reverse IxB cycle (-35 kA \times 10.9 T = 382 kN/m)
11. Final DC measurement ($B=10.9$ T, $T=10$ K)

During the initial cooldown (Step 1), the cables were expected to accumulate an additional $\sim 0.2\%$ axial strain due to the CTE differences in the special Invar clamps and the primarily copper cables as described in Section 3. Figure 6 shows experimental strain gauge data from the cooldown from room temperature to 5 K. The initial $\sim 0.3\%$ axial strain results from the invar shims inserted with the hydraulic jacks before installation in the SULTAN test well at room temperature. As the cables cool within the assembly to 5 K, an additional $\sim 0.2\%$ external axial strain is accumulated. Because the strain

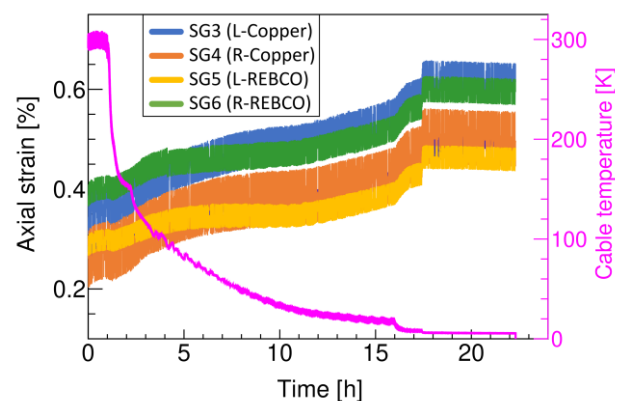


Figure 6: The measured increase in axial strain on the left cable (SG3, SG5) and right cable (SG4, SG6) during assembly cooldown in the SULTAN facility. The cable temperature is plotted on the right axis in magenta.

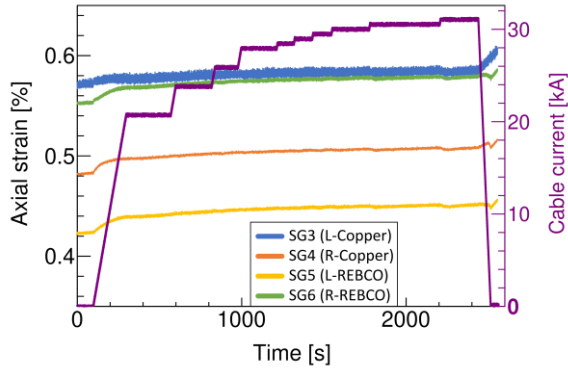


Figure 7: Measured axial strain on the left cable (SG3, SG5) and right cable (SG4, SG6) during one of the final current ramps after 500 IxB mechanical cycles. The cable current is plotted on the right axis in dark purple.

reference is on a small section of identical dummy cable, which is poorly thermally coupled to the rest of the assembly due to Teflon brackets, there is a slight time delay in the strain magnitude relative to cable temperature. This measurement confirms (1) that the dummy cable axially shrinks while the two clamped cables cannot, resulting in measured axial strain on the half bridges and (2) that the combination of mechanical and CTE strain combine to achieve an external axial strain of $\sim 0.5\%$ on the copper jacket.

We note that the measured strain increase due to CTE differences was $\sim 0.1\%$ less than the expected $\sim 0.3\%$ from calculations with perfect non-slip conditions and from the FEA simulations presented in Figure 3. This is explained by the frictional slip described in Section 3, which reduces the total effective strain on the cable when cooling down. However, once both the CTE-induced and hydraulic-induced strains are accounted for – and utilizing the FEA model presented in Section 3 to translate axial strain from the cable jacket to the REBCO stack – the measured $\sim 0.5\%$ jacket axial

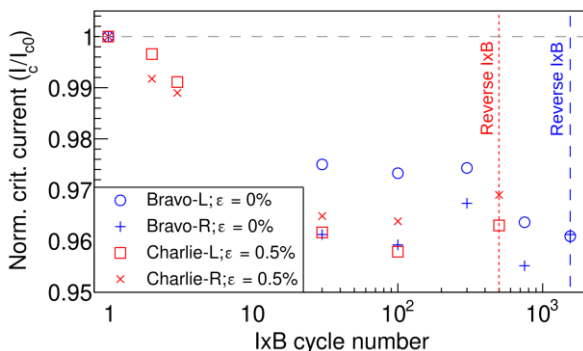


Figure 8: Critical current degradation for unstrained cables (Bravo) compared to 0.5% externally strained cables (Charlie). All 4 cables were identical with the exception of applied axial strain and IxB cycled at 382 kN/m at 5 K.

strain results in $\sim 0.3\%$ tape axial strain during the SULTAN test campaign. This is on the order of the maximum strain expected in high-field REBCO magnets, which are typically designed to be stress limited with axial strains on the conductor kept below 0.2%.

An example of strain gauge readouts during the final DC characterization (Step 11) is shown in Figure 7. This result is important for two reasons. First, strains remain effectively constant throughout the current ramp profile and subsequent IxB loading of the cable, with slight increase caused by electromagnetic forces on the lower cable-to-cable joint pulling the sample downward. Second, the initial axial strain was maintained throughout the entire test campaign, ensuring the IxB loading and strain were present simultaneously.

Critical current degradation as a function of IxB cycle number is shown for two unstrained (“Bravo” test) and two strained (“Charlie” test) VIPER cables in Figure 8. All four cables are identical in fabrication and were cycled identically at 10.9 T x 35 kA = 382 kN/m at 5 K. The initial reference critical currents for the “Charlie” test were 29.2 kA and 29.1 kA for cable A and B, respectively, as measured at 10.9 T and 10 K; the final critical currents at the end of the test campaign were 28.2 kA for both cables under the same magnetic field and temperature. The small initial degradation stabilized at less than 5% within approximately the first 30 IxB cycles. Importantly, there is no discernable difference in degradation between unstrained and strained cables, confirming the results obtained on single REBCO tapes (*e.g.* [12]) in a full-scale representative 96 tape per channel stacked and soldered cable. The results indicate that VIPER cables are robust to the realistic application of transverse loading and axial strain that would be experienced in high-field REBCO magnets.

Despite operating further into the SULTAN high-field region than is typical, due to the need for longer friction clamps in the joint region to ensure axial strain, the bottom cable-to-cable electrical joint achieved low resistance, measuring between 1.9 nΩ (5 K, 30 kA, 0 T) and 3.7 nΩ (10 K, 21 kA, 4.3 T average on joint). This corresponds to a normalized resistance per unit area of only 20–45 pΩm².

After the test campaign was concluded, the sample was warmed up and removed from the facility. Inspection of the sample shows that the Invar shims, which were tight at room temperature upon assembly installation in SULTAN, were now slightly loose. This indicates some further plastic deformation of the cables occurred during the initial stressing, which was expected from elastic-plastic FEA modeling of the cables in the assembly.

5. Conclusion

A novel method was demonstrated at the SULTAN facility to enable critical current testing of VIPER cables under simultaneous transverse IxB loading and axial mechanical strain on the REBCO stacks. The approach

required a specially designed test assembly that combined stress from hydraulic jacks implemented at room-temperature on the benchtop and from differential CTE between the Invar clamps and copper cable during sample cooldown in the SULTAN test well. Strain gauge measurements were consistent with detailed FEA modeling of the cables under axial load although implementation of anisotropic REBCO stack models as well as multiple elastic-plastic cycles could increase the model fidelity. Despite careful design, a small amount of friction slip occurred at the highest stress states in SULTAN, reducing the axial strain on the REBCO stacks from the target ~0.4% to ~0.3% during experiments. Reducing the friction clamp length in a future assembly would reduce this issue by extending the strained cable length.

Through the use of this assembly, VIPER cables were shown to be robust against critical current degradation from simultaneous transverse loading cycles at 382 kN/m and axial mechanical strain of ~0.3% in the REBCO stacks, in excess of the conditions expected in a high-field VIPER magnet. This approach allows relatively simple straight cables in existing test facilities such as SULTAN to achieve realistic high-field magnet test conditions that previously required testing single-layer 3D insert coils at rare and extensive facilities such as the ITER Test Facility (Naka, Japan) [26] or the NIFS 13 T large bore magnet facility (Toki City, Japan) [27]. The method described here results in faster superconducting cable and magnet development timelines with significantly reduced engineering resources.

Acknowledgements

The authors are indebted to the technical staff at MIT Plasma Science and Fusion Center for their work on fabrication, assembly, and shipping of the hardware described in this paper. We also wish to thank the SULTAN team at the Paul Scherrer Institut, especially Pierluigi Bruzzone, Boris Stepanov, Kamil Sedlak, Markus Jenni, and Christophe Müller for their tireless work and expert guidance during the cable test campaign. We also thank our research sponsors Commonwealth Fusion Systems who generously supported this work.

References

- [1] Z. S. Hartwig *et al.*, "VIPER: an industrially scalable high-current high-temperature superconductor cable," *Supercond. Sci. Technol.*, vol. 33, no. 11, p. 11LT01, Oct. 2020, doi: 10.1088/1361-6668/abb8c0.
- [2] G. Celentano *et al.*, "Design of an industrially feasible twisted-stack HTS cable-in-conduit conductor for fusion application," *IEEE Trans. Appl. Supercond.*, vol. 24, no. 3, 2014, doi: 10.1109/TASC.2013.2287910.
- [3] D. C. van der Laan, J. D. Weiss, and D. M. McRae, "Status of CORC® cables and wires for use in high-field magnets and power systems a decade after their introduction," *Supercond. Sci. Technol.*, vol. 32, no. 3, p. 033001, Feb. 2019, doi: 10.1088/1361-6668/aafc82.
- [4] T. Mulder, J. Weiss, D. van der Laan, A. Dudarev, and H. ten Kate, "Recent Progress in the Development of CORC Cable-In-Conduit Conductors," *IEEE Trans. Appl. Supercond.*, vol. 30, no. 4, pp. 1–5, Jun. 2020, doi: 10.1109/TASC.2020.2968251.
- [5] N. Bykovsky, D. Uglietti, K. Sedlak, B. Stepanov, R. Wesche, and P. Bruzzone, "Performance evolution of 60 kA HTS cable prototypes in the EDIPO test facility," *Supercond. Sci. Technol.*, vol. 29, no. 8, p. 084002, Jun. 2016, doi: 10.1088/0953-2048/29/8/084002.
- [6] N. Yanagi *et al.*, "Magnet design with 100-kA HTS STARS conductors for the helical fusion reactor," *Cryogenics*, vol. 80, pp. 243–249, Dec. 2016, doi: 10.1016/j.cryogenics.2016.06.011.
- [7] M. J. Wolf, W. H. Fietz, C. M. Bayer, S. I. Schlachter, R. Heller, and K.-P. Weiss, "HTS CroCo: A Stacked HTS Conductor Optimized for High Currents and Long-Length Production," *IEEE Trans. Appl. Supercond.*, vol. 26, no. 2, pp. 19–24, Mar. 2016, doi: 10.1109/TASC.2016.2521323.
- [8] P. Bruzzone *et al.*, "High temperature superconductors for fusion magnets," *Nucl. Fusion*, vol. 58, no. 10, p. 103001, Aug. 2018, doi: 10.1088/1741-4326/aad835.
- [9] N. Mitchell *et al.*, "Superconductors for fusion: a roadmap," *Supercond. Sci. Technol.*, vol. 34, no. 10, p. 103001, Sep. 2021, doi: 10.1088/1361-6668/ac0992.
- [10] D. C. van der Laan, J. W. Ekin, J. F. Douglas, C. C. Clickner, T. C. Stauffer, and L. F. Goodrich, "Effect of strain, magnetic field and field angle on the critical current density of Y Ba₂Cu₃O_{7- δ} coated conductors," *Supercond. Sci. Technol.*, vol. 23, no. 7, p. 072001, May 2010, doi: 10.1088/0953-2048/23/7/072001.
- [11] N. C. Allen, L. Chiesa, and M. Takayasu, "Combined Tension-Torsion Effects on 2G REBCO Tapes for Twisted Stacked-Tape Cabling," *IEEE Trans. Appl. Supercond.*, vol. 25, no. 3, pp. 1–5, Jun. 2015, doi: 10.1109/TASC.2014.2364401.
- [12] F. Pierro, M. Delgado, L. Chiesa, X. Wang, and S. O. Prestemon, "Measurements of the Strain Dependence of Critical Current of Commercial REBCO Tapes at 15 T Between 4.2 and 40 K for High Field Magnets," *IEEE Trans. Appl. Supercond.*, vol. 29, no. 5, pp. 1–5, Aug. 2019, doi: 10.1109/TASC.2019.2902458.
- [13] M. Takayasu, "Width-bending characteristic of REBCO HTS tape and flat-tape Rutherford-type cabling," *Supercond. Sci. Technol.*, vol. 34, no. 12, p. 125020, Nov. 2021, doi: 10.1088/1361-6668/ac30eb.
- [14] J. D. Weiss, T. Mulder, H. J. ten Kate, and D. C. van der Laan, "Introduction of CORC® wires: Highly flexible, round high-temperature superconducting wires for magnet and power transmission applications," in

- Superconductor science and technology*, Jan. 2017, vol. 30, no. 1, p. 014002. doi: 10.1088/0953-2048/30/1/014002.
- [15] A. Vostner, E. Salpietro, K. P. Weiss, W. H. Fietz, A. della Corte, and L. Muzzi, "The FBI Facility—a test rig for critical current measurements on CICC as a function of strain," *IEEE Trans. Appl. Supercond.*, vol. 15, no. 2, pp. 1387–1390, Jun. 2005, doi: 10.1109/TASC.2005.849097.
- [16] C. Bayer, C. Barth, P. V. Gade, K.-P. Weiss, and R. Heller, "FBI Measurement Facility for High Temperature Superconducting Cable Designs," *IEEE Trans. Appl. Supercond.*, vol. 24, no. 3, pp. 1–4, Jun. 2014, doi: 10.1109/TASC.2013.2287710.
- [17] A. Devred *et al.*, "Challenges and status of ITER conductor production," *Supercond. Sci. Technol.*, vol. 27, no. 4, p. 044001, Mar. 2014, doi: 10.1088/0953-2048/27/4/044001.
- [18] P. Bruzzone *et al.*, "Upgrade of operating range for SULTAN test facility," *IEEE Trans. Appl. Supercond.*, vol. 12, no. 1, pp. 520–523, Mar. 2002, doi: 10.1109/TASC.2002.1018457.
- [19] R. Wesche, P. Bruzzone, D. Uglietti, N. Bykovsky, and M. Lewandowska, "Upgrade of SULTAN/EDIPO for HTS Cable Test," *Phys. Procedia*, vol. 67, pp. 762–767, Jan. 2015, doi: 10.1016/j.phpro.2015.06.129.
- [20] P. Decool, D. Bessette, V. Cantone, and H. Cloez, "Investigation on Thermal Strain in Full Size ITER Conductors," *IEEE Trans. Appl. Supercond.*, vol. 18, no. 2, pp. 1097–1100, Jun. 2008, doi: 10.1109/TASC.2008.920551.
- [21] T. Hemmi *et al.*, "Test Results and Investigation of Tcs Degradation in Japanese ITER CS Conductor Samples," *IEEE Trans. Appl. Supercond.*, vol. 22, no. 3, pp. 4803305–4803305, Jun. 2012, doi: 10.1109/TASC.2011.2178370.
- [22] S. A. March *et al.*, "Results of the TFEU6 Sample Tested in SULTAN," *IEEE Trans. Appl. Supercond.*, vol. 23, no. 3, pp. 4200204–4200204, Jun. 2013, doi: 10.1109/TASC.2012.2228893.
- [23] "CRPP Annual Report - 1998," Ecole Polytechnique de Lausanne, Lausanne, Switzerland, Annual Research Summary, 1998.
- [24] M. Takayasu, L. Chiesa, L. Bromberg, and J. V. Minervini, "HTS twisted stacked-tape cable conductor," *Supercond. Sci. Technol.*, vol. 25, no. 1, p. 014011, Dec. 2011, doi: 10.1088/0953-2048/25/1/014011.
- [25] E. E. Salazar *et al.*, "Fiber optic quench detection for large-scale HTS magnets demonstrated on VIPER cable during high-fidelity testing at the SULTAN facility," *Supercond. Sci. Technol.*, vol. 34, no. 3, p. 035027, Feb. 2021, doi: 10.1088/1361-6668/abdba8.
- [26] S. Shimamoto *et al.*, "Construction of ITER common test facility for CS model coil," *IEEE Trans. Magn.*, vol. 32, no. 4, pp. 3049–3052, Jul. 1996, doi: 10.1109/20.511519.
- [27] S. Imagawa *et al.*, "Plan for Testing High-Current Superconductors for Fusion Reactors with A 15T Test Facility," *Plasma Fusion Res.*, vol. 10, pp. 3405012–3405012, 2015, doi: 10.1585/pfr.10.3405012.